

AD-A142 017

CRYSTALLINE-STATE EXTRUSION OF LOW DENSITY
POLYETHYLENES(U) MASSACHUSETTS UNIV AMHERST DEPT OF
POLYMER SCIENCE AND ENGINEERING C BENELHADJSAID ET AL.

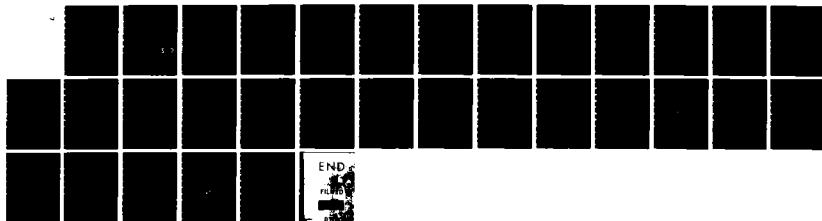
1/1

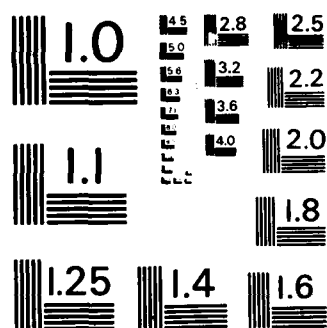
UNCLASSIFIED

15 AUG 83 TR-19 N00014-83-K-0228

F/G 13/8

NL





MICROCOPY RESOLUTION TEST CHART
NATIONAL BUREAU OF STANDARDS - 1963 - A

AD-A142 017

DTIC FILE COPY

Unclassified

12

| REPORT DOCUMENTATION PAGE | | READ INSTRUCTIONS BEFORE COMPLETING FORM |
|--|-----------------------|--|
| 1. REPORT NUMBER Technical Report No. 19 | 2. GOVT ACCESSION NO. | 3. RECIPIENT'S CATALOG NUMBER |
| 4. TITLE (and Subtitle) Crystalline-State Extrusion of Low Density Polyethylenes | | 5. TYPE OF REPORT & PERIOD COVERED Interim |
| | | 6. PERFORMING ORG. REPORT NUMBER |
| 7. AUTHOR(s) Chadli Benelhadjsaid and Roger S. Porter | | 8. CONTRACT OR GRANT NUMBER(s) N00014-83-K-0228 |
| 9. PERFORMING ORGANIZATION NAME AND ADDRESS Polymer Science and Engineering University of Massachusetts Amherst, Massachusetts 01003 | | 10. PROGRAM ELEMENT, PROJECT, TASK AREA & WORK UNIT NUMBERS |
| 11. CONTROLLING OFFICE NAME AND ADDRESS ONR Branch Office 666 Summer Street Boston, Massachusetts 02210 | | 12. REPORT DATE August 15, 1983 |
| | | 13. NUMBER OF PAGES |
| 14. MONITORING AGENCY NAME & ADDRESS (if different from Controlling Office) | | 15. SECURITY CLASS. (of this report) Unclassified |
| | | 15a. DECLASSIFICATION/DOWNGRADING SCHEDULE |
| 16. DISTRIBUTION STATEMENT (of this Report) Approved for public release; distribution unlimited | | |
| 17. DISTRIBUTION STATEMENT (of the abstract entered in Block 20, if different from Report) | | |
| 18. SUPPLEMENTARY NOTES | | |
| 19. KEY WORDS (Continue on reverse side if necessary and identify by block number) Low Density Polyethylene, Extrusion, Draw Ratio, Orientation | | |
| 20. ABSTRACT (Continue on reverse side if necessary and identify by block number) Three low density polyethylenes, one long branched (A) and two linear (B and C), have been solid-state extruded at several constant temperatures from ambient to 80°C and to draw ratios < 8. The initial densities and melt indices of A, B and C are 0.920, 0.920 and 0.935 g/cm ³ , and 1.9, 0.8 and 1.2 respectively. Melt-crystallized cylindrical billets were extruded through conical dies in an Instron Capillary Rheometer. The linear polymers were found to draw by extrusion more readily than the branched; all three strain-harden. Density, birefringence, | | |

DTIC
ELECTE
JUN 12 1984
S B

DD FORM 1473
1 JAN 73EDITION OF 1 NOV 65 IS OBSOLETE
S/N 0102-014-6601

Unclassified

84 06 11 006

SECURITY CLASSIFICATION OF THIS PAGE (When Data Entered)

Unclassified

tensile and thermal properties have been evaluated as functions of extrusion temperature and draw ratio. Despite a measured loss via die swell, substantial orientation takes place during solid-state extrusion as evidenced by increases in transparency, birefringence and tensile modulus (up to 4.5 times that of the original isotropic polymer). Depending on the polymer and the draw temperature, density does go through a minimum or shows a monotonic increase with draw by extrusion. A minimum in modulus is also observed at low draw and at all draw temperatures for all three polymers. The highest tensile moduli achieved are 0.73, 0.46 and 1.5 GPa for A, B and C respectively at their highest draw ratio. The melting point for polymer B decreases with extrusion draw ratio, whereas it remains constant after a small initial drop, for the two others. For all three low density polyethylenes, birefringence increases rapidly with extrusion draw and then levels off at high draw. The birefringence limit is similar for A and B, i.e. 0.046 ± 0.004 , but higher for C, i.e. 0.068 ± 0.009 . This work extends beyond others in that it studies the effect of short as well as long branches in solid-state extrusion by comparing the linear and long branched LDPE polymers and LDPE with prior evaluations of HDPE.

| | |
|--------------------|----------------------|
| Accession For | |
| NTIS GRA&I | ✓ |
| DTIC TAB | |
| Unannounced | |
| Justification | |
| By | |
| Distribution/ | |
| Availability Codes | |
| Dist | Avail and/or Special |
| A-1 | |

UTL
NOT
SELECTED

Unclassified

SECURITY CLASSIFICATION OF THIS PAGE(When Data Entered)

INTRODUCTION

The crystalline (solid) state extrusion of several thermoplastics has been studied extensively over this past decade for the purpose of producing anisotropic morphologies. Despite the fact that low density polyethylene (LDPE) is the largest volume thermoplastic in the world¹, it has been utilized in only a few such studies: note the solid state and hydrostatic extrusions by Buckley and Long² and by Alexander and Wormell³ respectively. The advent of linear LDPE resins has opened new opportunities for studying the effect of short as well as long branches in solid state extrusion. Thus, the purpose of this study is not only to evaluate the property changes achieved through uniaxial extrusion draw of three polyethylenes, but also to compare the linear and long branched LDPE polymers and also LDPE with prior evaluations of HDPE⁴⁻¹⁵. Consideration will also be given to the differences and similarities between solid-state extrusion and cold drawing in inducing high uniaxial orientation. Four principal methods of characterization were used: thermal analysis, density, tensile and birefringence measurements. The variables of draw were extrusion temperature and draw ratio. Additional properties such as die swell and transparency are considered.

EXPERIMENTAL

1. Polymer Materials

Three polyethylenes were used in this study: one long branched (LDPE) and two linear low density polyethylenes (LLDPE). Their properties, as provided by

the producers, are listed in Table 1. In the text, these polyethylenes are referred to as A, B and C. A is the polymer with long branches whereas B and C are linear polymers with short branches obtained in a low pressure reactor. The choice of these three polymers enables us to investigate the influence on the extrusion process and consequent polymer properties of:

(i) long chain branching, on comparing A and B which have the same crystallinity,

(ii) short chain branching content by comparing B and C which exhibit different fractional crystallinities.

We have also extended the comparison to high density polyethylene for which abundant information literature is available.

To estimate the polymer molecular weights, a relation (Equation 1) between the number average molecular weight (\bar{M}_n) and the melt flow index (MI) has been used. This correlation has been previously applied to low density polyethylenes¹⁶. As the density increases, number averages calculated from Equation 1 will err on the high side¹⁶. This means that the \bar{M}_n of polymer C is likely slightly lower than 34,000.

$$(\bar{M}_n)^{1/2} = 188 - 30 \log (MI) \quad (1)$$

2. Billet Preparation

The cylindrical billets to be extruded were prepared in the barrel of an Instron capillary rheometer. The original polymer was melted under a pressure P_c at a temperature T_1 above its melting point. To avoid the formation of

voids, it was then recrystallized by cooling while still under the same pressure P_c . The cooling rate did not exceed $1^\circ\text{C}/\text{min}$. The pressure was then released at a temperature T_2 below its ambient pressure melting point. The preparation conditions may be summarized:

Billet Preparation Conditions

| Polyethylene | P_c (MPa) | T_1 ($^\circ\text{C}$) | T_2 ($^\circ\text{C}$) |
|--------------|-------------|----------------------------|----------------------------|
| A | 150 | 172 | 80 |
| B | 64 | 162 | 85 |
| C | 64 | 162 | 85 |

3. Extrusion Draw Process

The extrusion was carried out in the Instron Rheometer at four different constant temperatures, all below the ambient melting point: room temperature, 40, 60 and 80°C for each of the three polymers. The billet was pushed through a brass conical die of entrance angle 20° at constant speed. The length-to-diameter (L/D) of the die capillary was kept at 2.0. The pressure, which varies with time, is chart recorded. The extrusion rate, which is used along with the Instron speed to determine the extrusion draw ratio, is determined by following the motion of the extrudate using a cathetometer. In order to keep the extruded strand straight, a small weight of ~ 260 g is attached to it. The tensile force developed is negligible compared to the extrusion pressure. A micrometer was

used to measure the extrudate diameter.

4. Measurements

The density of the extrudates was measured in a density gradient column using a mixture of water and isopropanol with calibrated glass floats at $(23 \pm 0.1)^\circ\text{C}$. The melting point and the heat of fusion were measured using a Perkin-Elmer DSC-2. The calculations were made by a TADS computer. Two standards - naphthalene and indium - were used for temperature calibration. All measurements for the three polymers were made at a heating rate of $10^\circ\text{C}/\text{min}$. The melting point (MP) was defined as the peak value of the fusion curve.

The tensile properties of polymers A, B and C, were measured by a relaxation modulus in tension instead of the conventional Young's modulus for the following reasons:

- (i) The initial region of the stress strain curve for these samples is not linear even at $\epsilon < 0.1\%$.
- (ii) Most of the extrudates are curved, adding uncertainty.
- (iii) Extrudates are linearly viscoelastic within an uncertainty of less than 15% for strains $\epsilon < 1\%$.

The relaxation moduli were measured by carrying out a ramp-loaded stress relaxation test¹⁷ on an Instron at room temperature using a strain gauge extensometer of 25 mm gauge length. The sample is stretched at a speed of 0.05 cm/min for 1 min. The machine is then stopped and the sample is allowed to relax while the strain is kept constant. The stress relaxation modulus is

calculated by dividing the stress recorded after 4 min of relaxation at the constant strain. The initial gauge length of all samples were 5 cm and the strain rate $\sim 10^{-4} \text{ sec}^{-1}$.

Birefringence was measured using a Zeiss Calspar tilting compensator with a Zeiss polarizing microscope and a white light source (5500 Å wavelength). The total birefringence Δn_T of the extrudates was evaluated from the following equation¹⁸:

$$\Delta n_T = \frac{R}{d} \cdot \lambda \quad (2)$$

where d is the sample thickness, R the retardation and λ the wavelength. Thin samples for testing were cut from the extrudates using either a razor blade (for polymer A) or a rotary microtome with glass knives (for polymers B and C). The second method induces some orientation effects¹⁸. Consequently, the uncertainty in the birefringence is as high as 20% at low draw ratios for samples B and C.

EXTRUSION CHARACTERISTICS

Our goal is to produce flawless extrudates at the highest possible draw ratios (DR) for the extrusion temperatures studied. At high extrusion ratio, the back pressure becomes so large that instabilities take place, giving rise to irregularities in the extrudates. The ratio between the entrance and the exit cross-sectional areas of the die expresses the extent of deformation and is referred to as the draw ratio (DR). The final product, re the extrudate,

is characterized by three parameters: DR, the temperature of extrusion, T_{ex} , and the plunger velocity. The draw ratio is related to strain by Equation 3 where l and l_0 are the lengths of respectively the extrudate and the billet:

$$\text{Strain } \epsilon = \ln \frac{l}{l_0} = \text{LNR} \quad (3)$$

There is a marked increase of extrusion pressure with strain. This increase is particularly steep at low temperatures of extrusion. The same trend has been observed during hydrostatic extrusion of linear PE by Cappaccio et al.¹⁹ and by Takayanagi²⁰ who interpreted it as a strain-hardening phenomenon. Strain-hardening is an indication of the change in polymer structure from lamellar to fibrillar. Hence, more strain hardening means that more crystal bridges or tie molecules are formed during plastic deformation²⁰. At lower temperatures, the deformation efficiency is higher - i.e. less viscous dissipation - and strain hardening sets in earlier. The linear low density polyethylenes (B and C) draw more easily than the one with long branches (A). The extrusion velocities for the former are five times higher than that for the latter with the extrusion pressures of the same order. Long chain branching probably accounts for this large difference since the fractional crystallinity is the same in A and B - i.e. similarity in short chain branch content - and the molecular weight is lower in the former. Polymer C strain-hardens more readily than B of lower crystallinity (59% and 49% respectively). Polymer B has a higher short branches content and a higher molecular weight (34,000 and 36,000 respectively). Both large side groups and molecular weights reduce plastic deformation rates²¹.

Consequently, the transformation from lamellar to fiber structure takes place more readily in C than in B, thus explaining the more rapid strain hardening in the former^{19,20}.

The onset of flaws in extrudate is usually associated with instabilities in the pressure which starts fluctuating in a sinusoidal fashion. The more pronounced the fluctuations, the more severe the flaws in the extrudate.

There is an increase in optical transparency with DR. This is associated with higher orientation at higher draw ratio. Polymers A, B and C can be satisfactorily extruded in a single stage to draw ratios of respectively 6.0, 7.0 and 8.0 over the temperature range studied before severe flaws occur. Similar limitations have been observed for LDPE by Buckley and Long² and by Alexander and Wormell³. The latter attribute the cracks observed to melt fracture. Hope et al.²² concludes that the instabilities are caused by partial melting. The authors explain this by a temperature rise due to heat of deformation. Shear failure under compression is more likely the cause, cracks propagate helicoidally at ~ 45°C.

The expansion of the extrudate at the exit of the die, or Die Swell, is defined as follows:

$$D.S.(%) = \frac{d-d_0}{d_0} \times 100\% \quad (6)$$

where d and d_0 are the diameters of the extrudate and the die capillary respectively. Die swell as a function of temperature is plotted in Figure 2.

Die swell is a measure of the recovery of the elastic energy stored in both the capillary and its entrance zone²³. Since this expansion occurs below the

melting point and above T_g , die swell represents the elastic recovery of the amorphous component. Therefore, die swell in solid-state extrusion is small as compared to that in melt extrusion. Thus, the amount of die swell depends on the mobility of the amorphous chains, i.e. their ability to shrink back under ambient pressure and extension temperature.

Die swell for samples A and B goes through a minimum with increasing extrusion temperature whereas for C it simply decreases over the range studied. The same behavior as that of A and B is observed by Alexander and Wormell³ for LDPE. This behavior may be the result of two competing effects: the increased mobility of the chains on the one hand and the reduced deformation efficiency on the other hand.

Below the temperature of minimum swell, elastic recovery decreases with increasing draw ratio. Comparable observations have been made on both low² and on high density PE²². In the extrusion-drawn polymer, the tie molecules are taut and tend to relax upon release of the stress at the exit of the die. However, their mobility is more efficiently blocked and a portion may be crystalline as the extrusion draw ratio is increased^{24,25,26}.

The nominal draw ratio, i.e. die area ratio, (DR), is usually larger than the effective draw ratio, that is the extrusion draw ratio (EDR), because of die swell. The latter is a loss of orientation. Since we want to correlate extrudate properties to the actual extent of deformation, all measured properties will be reported as a function of EDR instead of DR. EDR was determined by the ratio of cross-sections of the billet and the extrudate.

PROPERTIES

Using a two-phase model, the degree of crystallinity was computed from density according to the following equation²⁷

$$\chi_c = \text{Crystallinity (\%)} = \frac{\rho_c}{\rho} \cdot \frac{\rho - \rho_a}{\rho_c - \rho_a} \times 100 \quad (10)$$

ρ = Measured density (g/cm³)

ρ_c = Crystalline density = 1.000 g/cm³(28)

ρ_a = Amorphous density = 0.855 g/cm³(28)

The changes in overall apparent crystallinity with extrusion draw are small i.e. < 4%. Density as a function of extrusion temperature and draw ratio is shown in Figure 3 for Sample B. The density goes through a minimum with increasing draw ratio for all three polymers and for all draw temperatures except at 60°C and 80°C for sample A and 80°C for B. A minimum in density is also reported by DeCandia et al.²⁹ for cold drawing of LDPE.

Chuah et al.⁸ observed density minima with draw for solid-state extrusion of HDPE. They explain it by the combination of two opposing processes: the crystalline density decreases while the amorphous density increases with draw, in accord with Glenz et al.³⁰. At high draw, the amorphous density becomes the determining factor. Hence, the larger the amorphous content - i.e. the lower the degree of crystallinity - the larger the effect on macroscopic density. Table 2 shows that the increase in density is dependent upon the crystallinity of the undrawn material. At higher extrusion temperatures, annealing becomes significant. Above the temperature at which the density decrease ceases,

crystals of more perfection may be produced by the combination of annealing and high draw and thus may also contribute to the density increase. In any case, at higher draw temperatures, a real increase in crystallinity is observed.

Using the same two-phase model as for crystallinity from density, one can calculate the apparent percent crystallinity knowing the heat of fusion, as determined from the area of the fusion curve. The degree of crystallinity in percent is defined as follows:³¹

$$\% \text{ Crystallinity} = \frac{\Delta H}{\Delta H_u}$$

where ΔH is the heat of fusion of the partially crystalline specimen and ΔH_u the heat of fusion of the perfect crystal.

The values are computed using a value of 69.2 cal/g for ΔH_u ^{10,15}. There are no appreciable changes in crystallinity with either draw ratio or extrusion temperature for all three polymers except for polymer A at DR = 7.0; B at DR = 7.0, 8.0 and C at DR = 9.0 at a temperature extrusion of 80°C. Despite the large deviations, i.e. up to 13%, between the values of crystallinity determined from heat of fusion and those from density, the two methods still show comparable trends. The large difference between crystallinities from density and heat of fusion stems most likely from the fact that the value 69.2 cal/g is too high for LDPE. The increase in crystallinity at higher extrusion draw and temperature support the previous conclusion.

The melting point is designated by the peak value of the fusion curve.

Figure 1 intercompares this melting point as a function of extrusion draw ratio for the three polymers extruded at 80°C. The melting point for samples A and C drops at EDR > 2.0 and then remains constant. For B, MP decreases regularly with extrusion draw. There is, though, little temperature dependence of MP.

The melting of low density polyethylenes as a function of extrusion draw differs markedly from that of HDPE for which the melting point is reported to increase modestly with draw^{9-11,32-34}. Buckley and Long² also observed no appreciable change in the melting points for LDPE.

Just as for drawn HPDE,^{9,12,34,35} our polymers seem also to superheat. Polymer A extruded at DR = 6.0 and T = 40°C is shown as an example:

| Scanning Rate (°C/min) | MP (°C) |
|------------------------|---------|
| 10 | 109 |
| 40 | 113 |
| 80 | 121 |

These values have not been corrected for the instrument lag. Yet, they are still lower than those reported by Mead³⁵ for HDPE, i.e. ~ 20°C increase in MP going in scanning rate from 10 to 80°C/min. This may mean that superheating effects of LDPE are small compared to those of HDPE. Double melting peaks are a notable characteristic of the fusion curves, especially for polymer B, see Figure 5. However, their appearance is not reproducible, nonetheless there are trends in melting behavior: irregularities in the endotherm shape showing up on EDR ~ 3.0, with the most conspicuous feature being an increasing sharpness and

smoothness of the melting peak at higher draw. Multiple melting peaks for drawn PE^{13,14,32,36,37} and other polymers^{38,39} have been reported.

The tensile modulus, E , varies similarly with EDR for all three low density polyethylenes. After going through a minimum at near EDR = 2, the modulus increases markedly with extrusion draw. The overall increase is up to 4.5, 2.5 and 4.0 times that of the original isotropic polymers for A, B, and C respectively. There is also a minor but clear dependence of modulus on extrusion temperature. At higher extrusion draw ratios and for the lower crystallinity polymers, A and B, E decreases with increasing extrusion temperature. Polymer A (Figure 6) shows the most rapid increase in modulus with draw. Although undrawn A has a lower modulus, it reaches a higher value than its linear counterpart B. That C reaches higher values than the former stems more from its higher ductility at these conditions than from its higher crystallinity.

The effect of extrusion draw on tensile modulus for LDPE differs from that for HDPE¹¹. In the latter case, the modulus increases slowly at draw ratios less than 10-15 whereas at higher draw ratios, the modulus increases rapidly and linearly with extrusion draw. The minimum in modulus at low EDR was not observed, in accord with Buckley and Long², who also found only a slight increase in tensile modulus on solid-state extrusion of LDPE. Our results also compare well with those for cold-drawn LDPE⁴⁰⁻⁴² including the anomalous pattern of the minimum modulus which seems to be unique to low density polyethylene⁴³. The highest moduli attained are shown in Table 3 which also includes the

highest moduli reported in literature⁴²⁻⁴⁸.

An explanation for the minimum has been given by Frank et al.⁴⁵ on the basis of two mechanisms: c-shear process and twin boundary migration. The c-axis shear mechanism is related to the mobility of the structure arising from an appreciable branch content which also gives rise at room temperature to a low shear modulus on planes along and perpendicular to the draw direction⁴⁶. Ward⁴⁸ showed that the mechanical anisotropy of LDPE is well predicted by the aggregate model.

Birefringence has been chosen to assess the extent of orientation during solid state extrusion of low density polyethylenes because it may be directly related to the permanent strain⁴². Birefringence is the difference between refractive indices along and perpendicular the draw direction. As the chain becomes more oriented, birefringence Δn increases as defined by the following equation⁴²:

$$\Delta n = \Delta n_{\max} (1 - \frac{3}{2} \overline{\sin^2 \theta}) \quad (12)$$

where Δn_{\max} is the maximum birefringence of full orientation and θ the angle between the chain axis and the draw direction. According to Equation 12, Δn initially rises sharply with increasing draw ratio and then turns plateaus at high draw⁴⁸. This is indeed what we observe for our low density polyethylenes, see Figure 7.

From Figure 7, we can see that within precision, A and B are indistinguishable, whereas C, of higher crystallinity, reaches higher values of

birefringence: 0.068 ± 0.009 . This value may be higher than any other previously reported for PE but the large uncertainty limits the significance of this result. In any case, this value is comparable with those obtained for ultradrawn HDPE fibers¹¹: 0.062 ± 0.002 . The highest value in birefringence for polymer A is 0.046 ± 0.004 at EDR = 4.9 and extrusion temperature $T_{ex} = 22^\circ\text{C}$ which is comparable to that of cold-drawn LDPE^{47,49,50}. Also, both extruded and cold drawn LDPE show the same pattern in birefringence change with draw. Therefore, it seems that birefringence is not influenced by long branching at least not within the precision of our results. There is a small but clear extrusion temperature dependence of birefringence in the case of polymer A but not in that of B or C perhaps because of the large uncertainty. The higher birefringence at lower draw temperature may be explained in terms of higher draw efficiency. The lower the temperature of draw and the higher the fraction of energy input that is stored elastically²³.

ACKNOWLEDGEMENT

This work was supported in part by the Office of Naval Research.

References

1. H. Ulrich, "Introduction to Industrial Polymers", Hanser, New York (1981).
2. A. Buckely and H.A. Long, Polym. Eng. Sci., 9, 115 (1969).
3. J.M. Alexander and P.J.H. Wormell, Annals. C.I.R.O., XIV, 21 (1971).
4. N. Capiati, S. Kojima, W. Perkins and R.S. Porter, J. Mater. Sci., 12, 334 (1977).
5. W.T. Mead and R.S. Porter, J. Polym. Sci., Polym. Symp., 63, 289 (1978).
6. S. Kojima and R.S. Porter, J. Appl. Polym. Sci., Appl. Polym. Symp., 33, 129 (1978).
7. W.G. Perkins, N.J. Capiati and R.S. Porter, Polym. Eng. Sci., 16, 200 (1976).
8. H.H. Chuah, R.E. DeMicheli and R.S. Porter, J. Polym. Sci., Polym. Lett. 21, 791 (1982).
9. J.H. Southern, R.S. Porter and H.E. Blair, J. Polym. Sci., A-2, 10, 1135 (1972).
10. S. Kojima, C.R. Desper and R.S. Porter, J. Polym. Sci., Polym. Phys. Ed., 16, 1721 (1978).
11. A.E. Zachariades, W.T. Mead and R.S. Porter, "Ultra-High Modulus Polymers", A. Ciferri and I.M. Ward (Editors), Applied Science, Essex, England (1979).
12. N.E. Weeks and R.S. Porter, J. Polym. Sci., Polym. Phys. Ed., 13, 2049 (1975).
13. J.H. Southern and R.S. Porter, J. Macromol. Sci.-Phys., B4, 541 (1970).

14. W.T. Mead and R.S. Porter, Intern. J. Polym. Mater., 7, 29 (1979).
15. J.H. Southern and R.S. Porter, J. Appl. Polym. Sci., 14, 2305 (1970).
16. D.J.H. Sandiford and A.H. Wilbourn, "Polyethene", A. Renfrew and P. Morgan (Editors), Iliffe and Sons, London (1960).
17. R.J. Farris, M.S. Thesis, University of Utah (1969).
18. G.L. Wilkes, J. Macromol. Sci.-Chem., C10, 149 (1974).
19. G. Cappaccio, A.G. Gibson and I.M. Ward, "Ultra High Modulus Polymers", A. Ciferri and I.M. Ward (Editors), Applied Science, Essex, England (1979).
20. M. Takayanagi, "Deformation and Fracture of High Polymers", H.H. Kausch, J.A. Hassell, R.I. Jaffee (Editors), Plenum Press, (1972).
21. P.S. Hope and B. Parsons, Polym. Eng. Sci., 20, 597 (1980).
22. P.S. Hope and B. Parsons, Polym. Eng. Sci., 20, 589 (1980).
23. R.S. Porter, "Exploring the Limits of Polymer Properties: Preparation Methods and Evaluation", NSF proposal.
24. F. DeCandia, R. Russo, V. Vittoria and A. Peterlin, J. Polym. Sci., Polym. Phys. Ed., 20, 1175 (1982).
25. R.S. Porter, personal communication.
26. A. Tsuruta, T. Kanamoto, K. Tanoka and R.S. Porter, unpublished.
27. J. Shultz, "Polymer Materials Science", p. 210, Prentice-Hall, New Jersey (1974).
28. J. Brandrup and E.H. Immergut, "Polymer Handbook", p. VI 4H, Interscience Publishers, New York (1967).

29. F. DeCandia, R. Russo, V. Vittoria and A. Peterlin, J. Polym. Sci. Polym. Phys. Ed., 20, 269 (1982).
30. W. Glenz, N. Morosoff and A. Peterlin, J. Polym. Sci. Polym. Lett., 9, 211 (1971).
31. P. Meares, "Polymers: Structure and Bulk Properties", Chapter 5, Van Nostrand Reinhold, London (1965).
32. S.M. Aharoni and J.P. Sibilis, J. Appl. Polym. Sci., 23, 133 (1979).
33. P.S. Hope, A.G. Gibson and I.M. Ward, J. Polym. Sci. Polym. Phys. Ed., 18, 1243 (1980).
34. J. Clements, G. Capaccio and I.M. Ward, J. Polym. Sci. Polym. Phys. Ed., 7, 693 (1979).
35. W.T. Mead and R.S. Porter, J. Appl. Phys., 47, 4278 (1976).
36. D.P. Pope, J. Polym. Sci. Polym. Phys. Ed., 14, 811 (1976).
37. L. Koski, J. Thermal Anal., 13, 467 (1978).
38. J.P. Bell and J.H. Dumbleton, J. Polym. Sci., A-2, 7, 1033 (1969).
39. G.E. Sweet and J.P. Bell, J. Polym. Sci., A-2, 10, 1273 (1972).
40. F. DeCandia, R. Russo, V. Vittoria and A. Peterlin, J. Polym. Sci., Polym. Phys. Ed., 20, 269 (1982).
41. F. DeCandia, A. Perullo, V. Vittoria and A. Peterlin, J. Appl. Polym. Sci., 28, 1815 (1983).
42. I.M. Ward, "Mechanical Properties of Solid Polymers", Chapter 10, Wiley, London (1971).

43. V.B. Gupta, A. Keller and I.M. Ward, J. Macromol. Sci. Phys., B2, 139 (1968).
44. D.W. Hadley, P.R. Pinnock and I.M. Ward, J. Mater. Sci., 4, 152 (1969).
45. F.C. Frank, V.B. Gupta and I.M. Ward, Phil. Mag., 21, 1127 (1970).
46. V.B. Gupta and I.M. Ward, J. Macromol. Sci. Phys., B2, 89 (1968).
47. V.B. Gupta and I.M. Ward, J. Macromol. Sci. Phys., B1, 373 (1967).
48. I.M. Ward, J. Polym. Sci. Polym. Symp., 58, 1 (1977).
49. S. Hoshino, J. Powers, D.G. Legrand, H. Kawai and R.S. Stein, J. Polym. Sci., 58, 185 (1962).
50. R.S. Stein and F.H. Norris, J. Polym. Sci., 21, 381 (1956).

Table 1
Characteristics of Polyethylene Samples Studied

| Sample | Type | Grade | Manufacturer | ρ , g/cm ³ | MI* | \bar{M}_n ** | Crystallinity (%)*** |
|--------|-------|------------|--------------|-------------------------------|-----|----------------|-------------------------|
| A | LDPE | Alathon 20 | duPont | 0.920 | 1.9 | 32,000 | 49 |
| B | LLDPE | FW 1290 | CdF Chimie | 0.920 | 0.8 | 36,000 | 49 |
| C | LLDPE | FW 1180 | CdF Chimie | 0.935 | 1.2 | 34,000 | 59 |

*ASTM D 1238, Melt Index.

**Calculated from Equation 1.

***Calculated from density.

Table 2
Overall Density Change

| Sample | Crystallinity (%) [*] at EDR = 1.0 | T _{ex} (°C) | EDR _{max} | Δρ(g/cm ³) ^{**} |
|-----------------------|--|----------------------|--------------------|--------------------------------------|
| A | 51 | 80 | 5.6 | +0.0034 |
| B | 52 | 80 | 6.4 | +0.0044 |
| C | 61 | 80 | 7.6 | +0.0019 |
| HDPE 1 ^{***} | 74 | 90 | 14 | -0.002 |
| HDPE 2 ^{***} | 82 | 100 | 16 | -0.005 |

^{*}From Equation 10.

^{**}Δρ = ρ(EDR_{max}) - ρ(EDR = 1.0).

^{***}HDPE samples showing a minimum in density with draw. Data from ref. 8.

Table 3
Presently Achievable Tensile Moduli of Polyethylene[†]

| Sample | Density (g/cm ³) | EDR _{max} | E(GPa) | Reference |
|--------|------------------------------|--------------------|--------|----------------------------------|
| A | 0.920 | 4.9 | 0.73 | -- |
| B | 0.920 | 5.5 | 0.46 | -- |
| C | 0.935 | 6.9 | 1.5 | -- |
| LDPE* | --- | 6.0 | 0.83 | Hadley et al. ⁴⁴ |
| LDPE* | 0.915 | 6.0 | <0.75 | DeCandia et al. ⁴¹ |
| LLDPE* | 0.914 | 8.0 | 1.1 | DeCandia et al. ⁴¹ |
| HDPE** | --- | 40 | 70 | Zachariades et al. ¹¹ |

*Cold drawn.

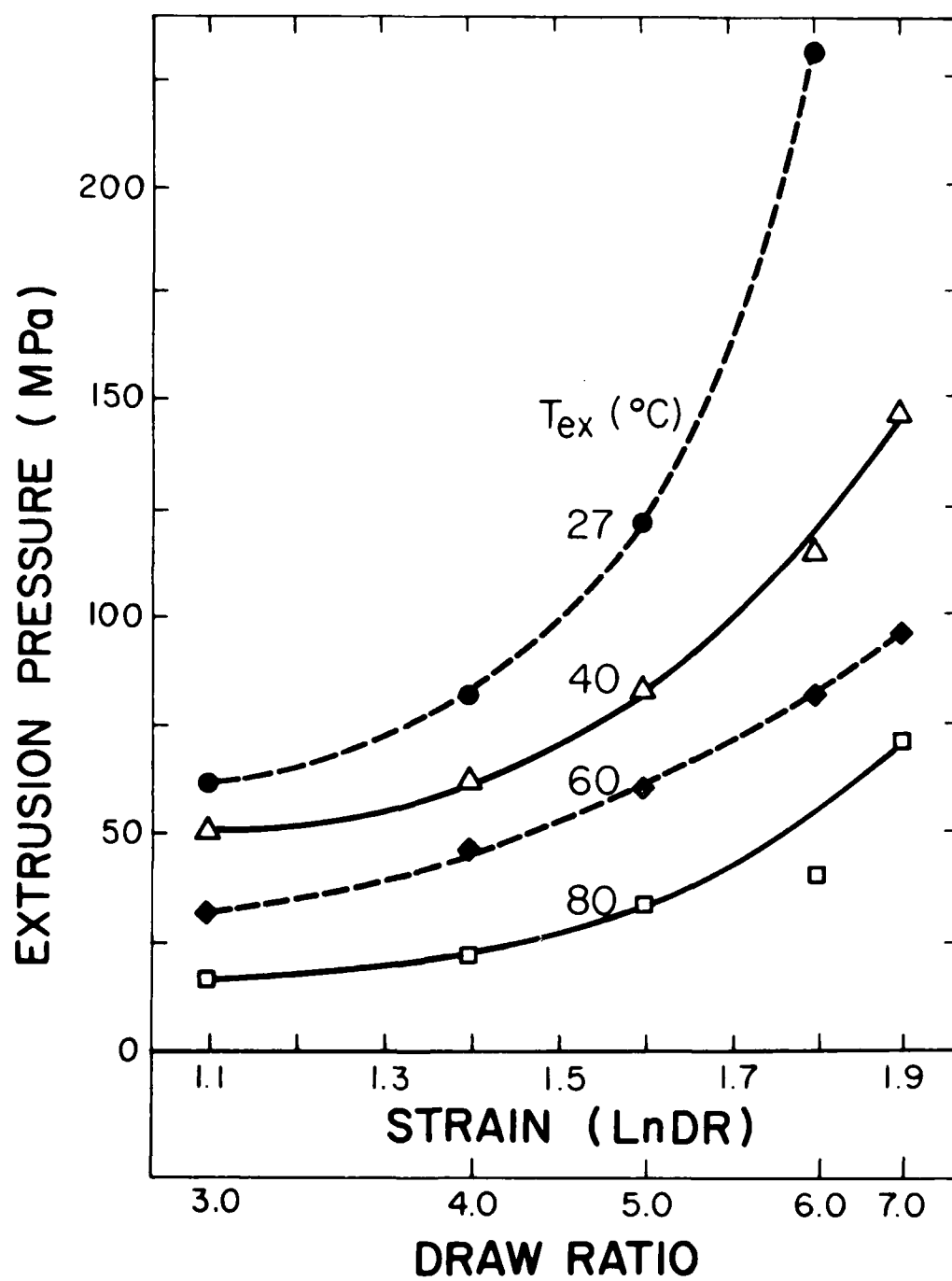
**Solid state extruded.

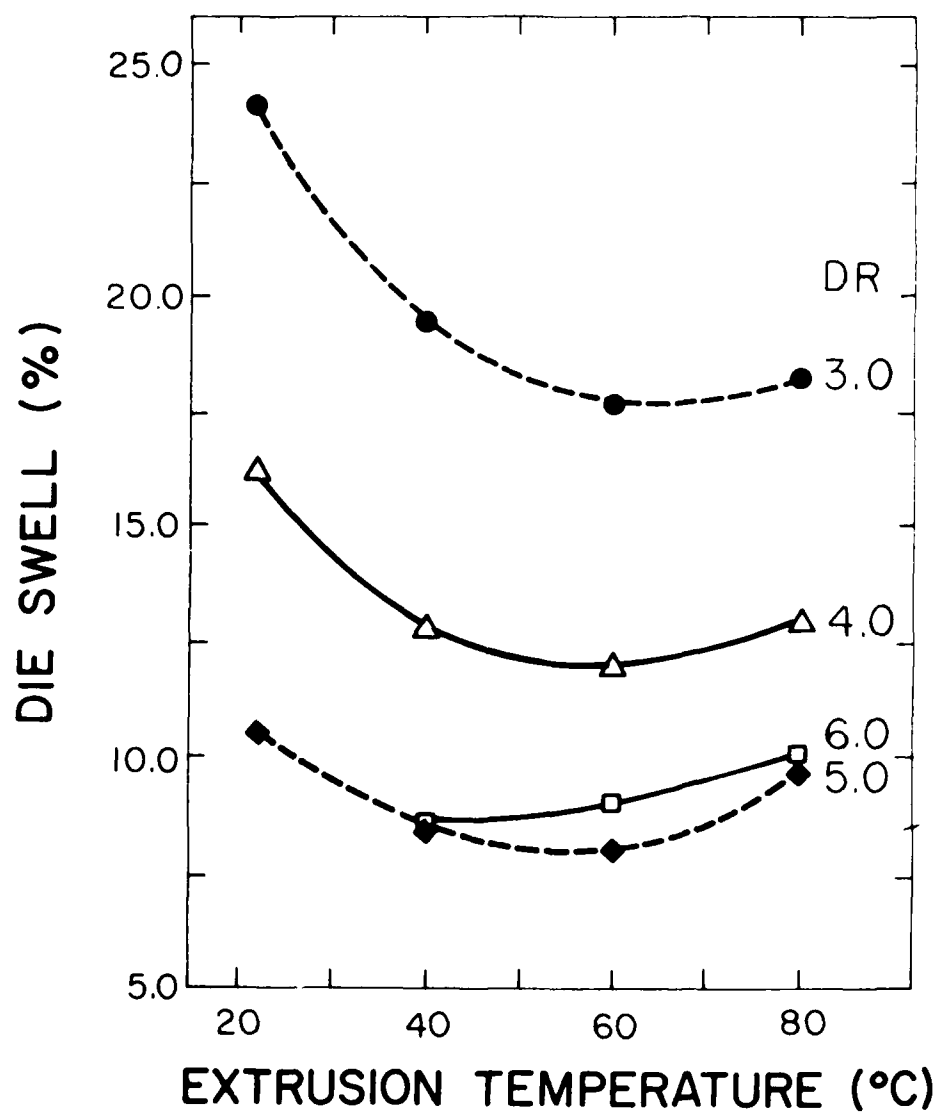
[†]Highly drawn by a very specialized technique, UHMWPE, with a special initial morphology, was found to exhibit ultra high tensile modulus, i.e. 222 GPaa.

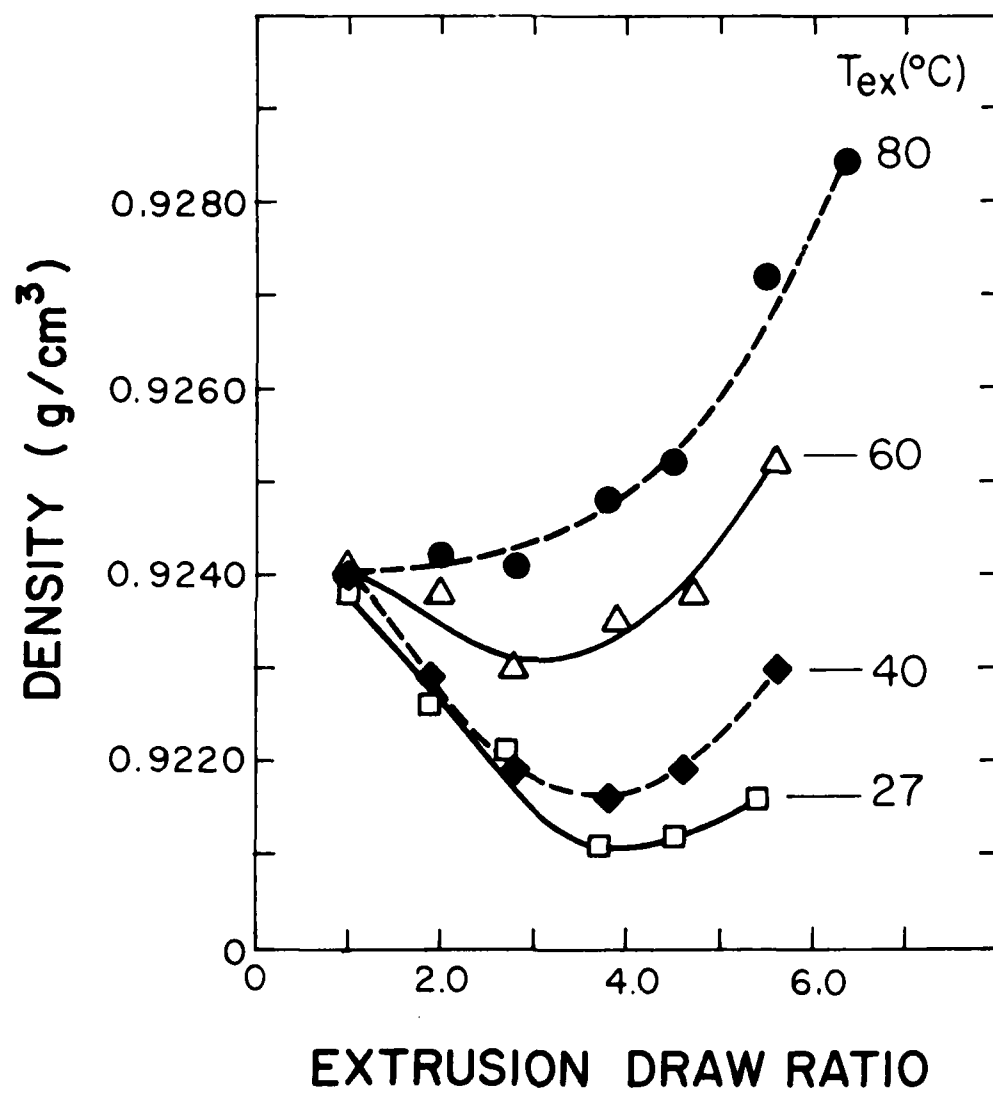
^aReference: T. Kanamoto, A. Tsuruta, K. Tanaka, M. Takeda and R.S. Porter, Polym. J., 15, 327 (1983).

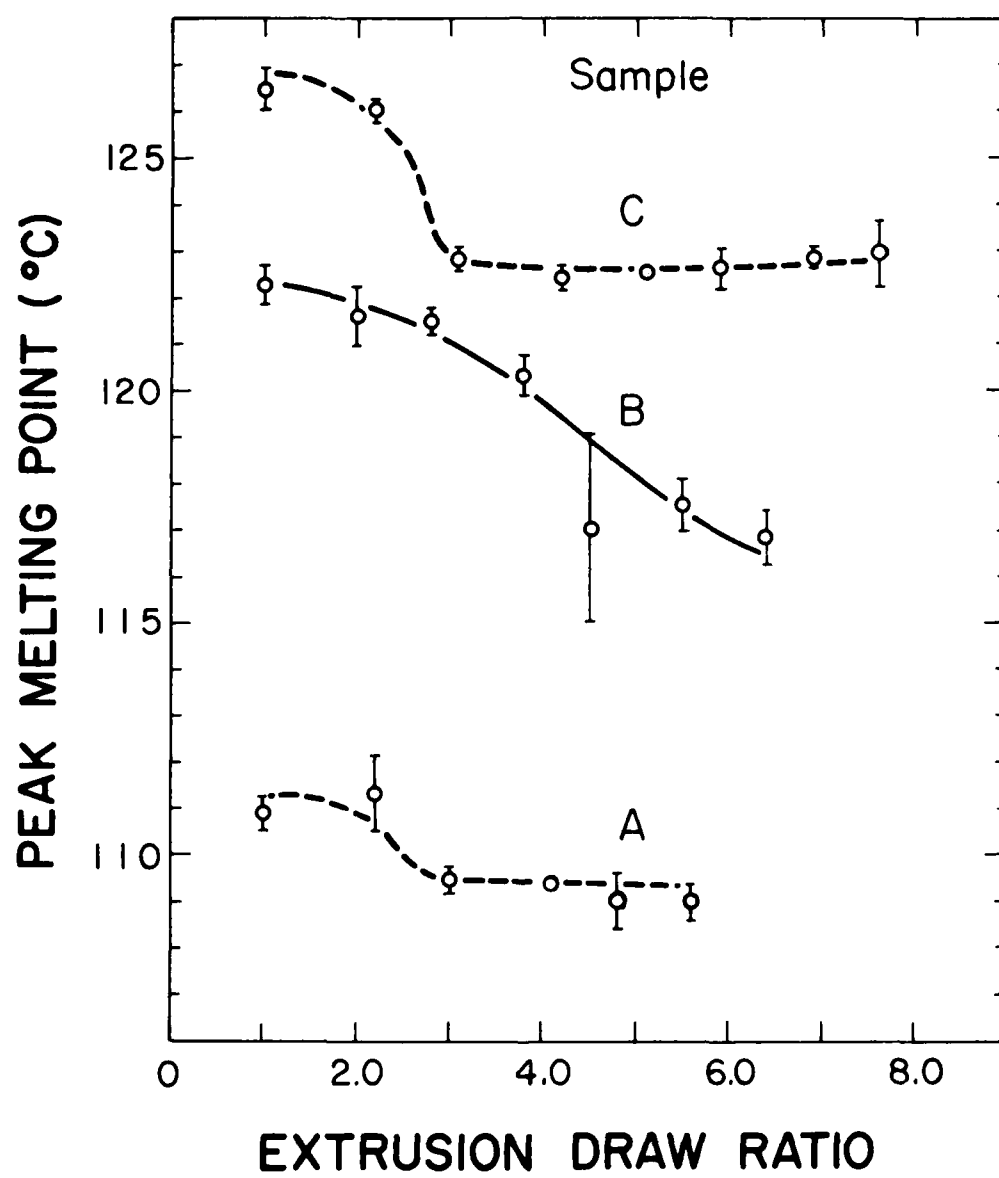
Figure Captions

- Figure 1. Sample C extrusion pressure versus strain at indicated extrusion temperatures.
- Figure 2. Extrudate die swell for sample A versus extrusion temperature for the draw ratios shown.
- Figure 3. Density of sample B extrudates versus EDR at the extrusion temperatures shown.
- Figure 4. Peak melting versus EDR for samples A, B and C extruded at 80°C.
- Figure 5. DSC endotherms for sample B extruded at 80°C at indicated EDR.
- Figure 6. Tensile modulus versus EDR for sample A. $T_{ex}=22$ (\blacktriangle); 40 (\bullet); 60 (\square); 80°C (\blacklozenge).
- Figure 7. Birefringence versus EDR for samples A (Δ), B (\blacksquare) and C (O) extruded at room temperature.

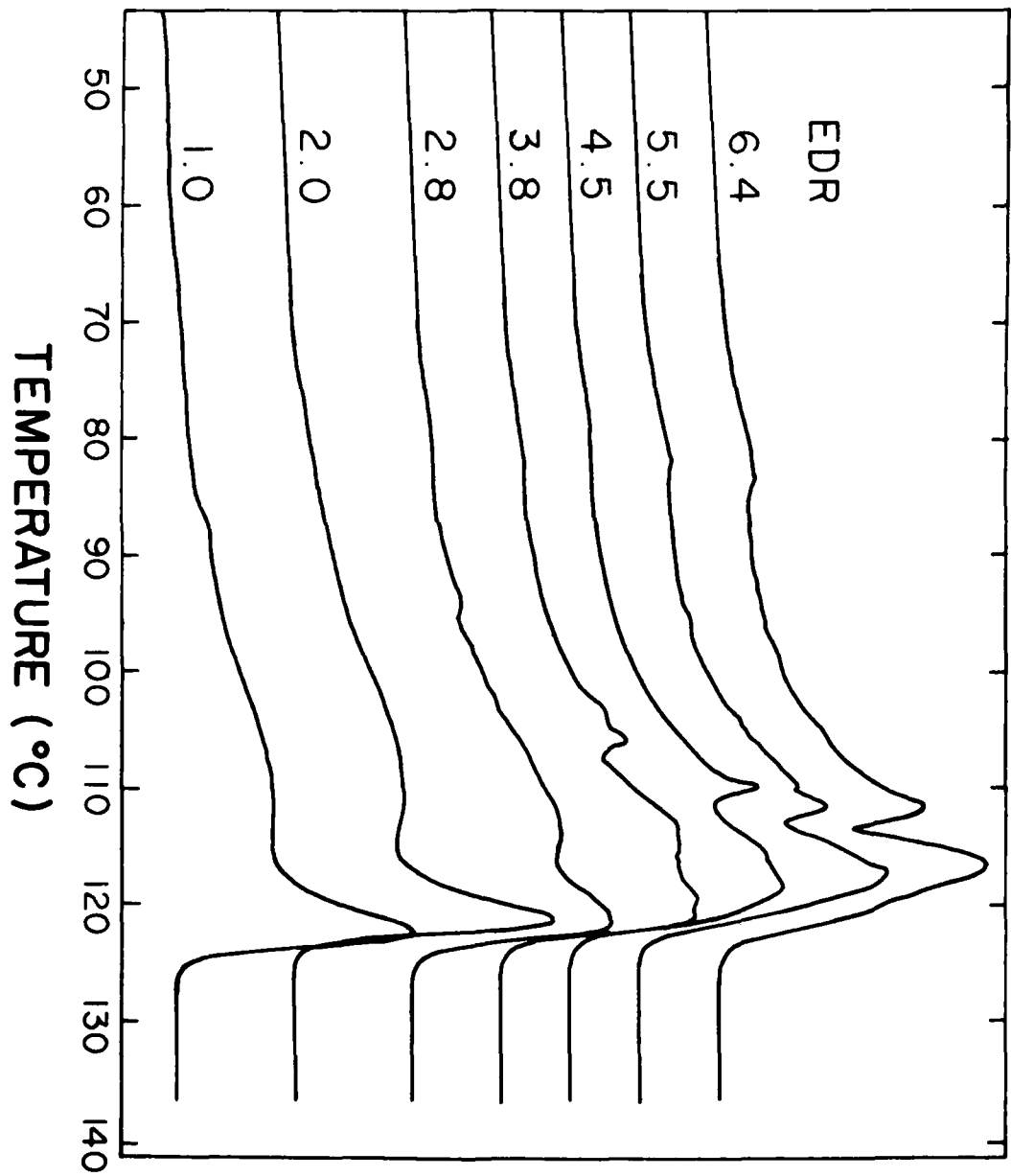


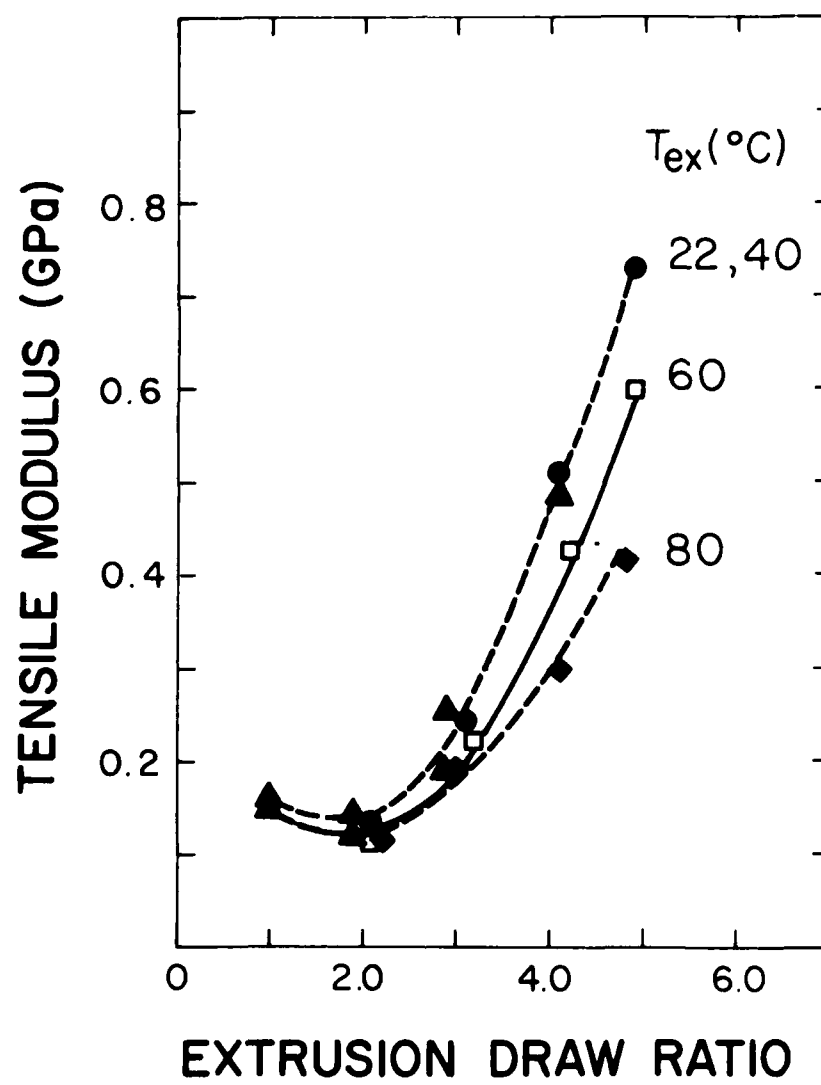


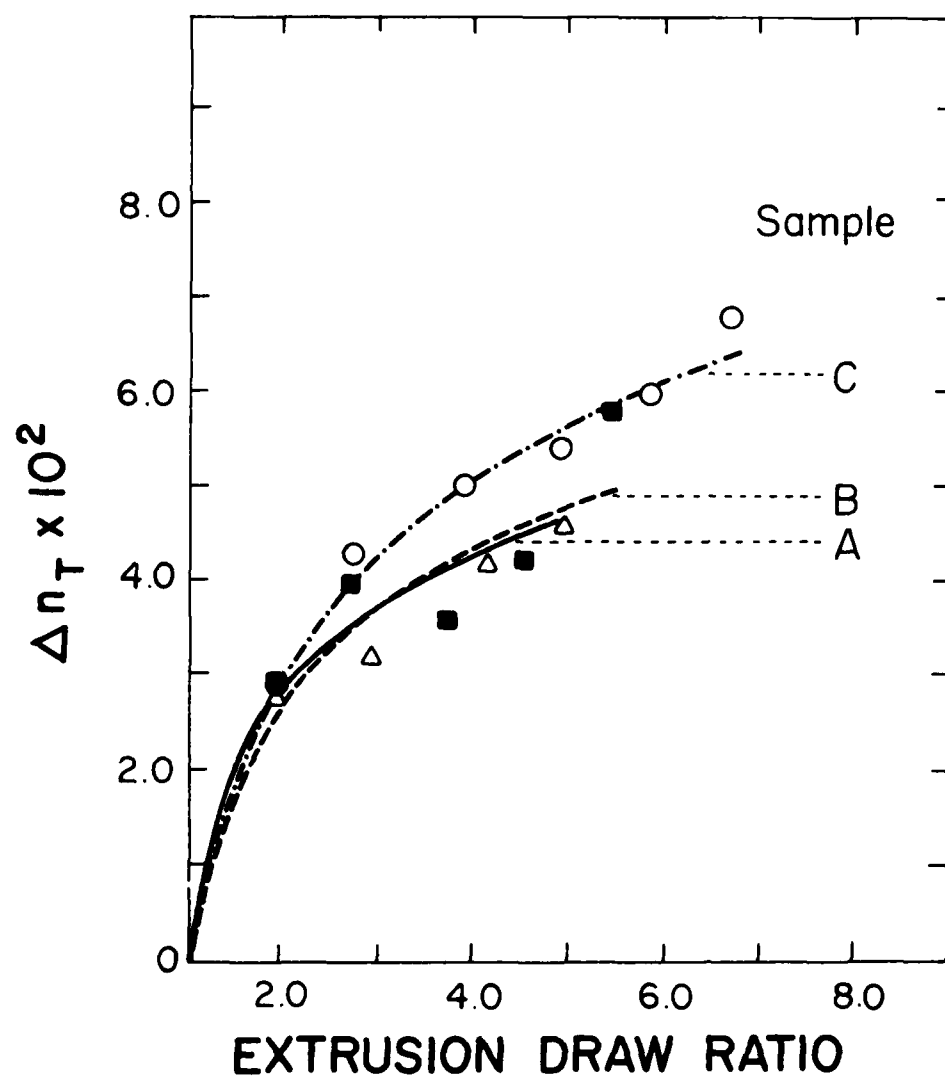




ENDOTHERM →







END

FILMED

7-84

DTIC